Local Air Entrainment and Detrainment

H. Kobus

Institut für Wasserbau, Universität Stuttgart, Federal Republic of Germany

I INTRODUCTION

Air and water are usually well separated by gravity due to their extreme difference in specific weight. Whenever they are mixed, however, they give rise to a very complex two-phase flow situation. The hydraulic engineer is often faced with the problem of estimating the effects of entrained air upon the flow, because this may be essential for the safe operation of a hydraulic structure. Depending upon the situation, air entrainment may be desirable, e.g. for cavitation prevention or oxygenation purposes, or undesirable, e.g. at intake structures or pump sumps.

The predominant mechanism in generating air-water mixtures is the inclusion of air at the surface of flowing water. The mechanics of free-surface flow may lead to ambient surface aeration in high-speed flows, or - even at moderate flow velocities - to flow configurations with localized air entrainment, which includes inadvertent self-aeration as well as such specific flow systems in which surface aeration is forced /13/.

For any given flow configuration causing local air entrainment, the following questions have to be answered:

- How much air is entrained by the system as a whole (Q_a), how much per unit length or width (q_a), and what is the resulting bubble size distribution? This will depend primarily upon the entraining mechanism and the given limitations.

- What is the relative motion of the air bubbles and the resulting air concentration distribution? How does the presence of the air influence or change the water flow? This will depend upon the distribution of bubble sizes as well as upon the turbulence characteristics of the flow, where one can distinguish bubble-induced turbulence, free shear turbulence and wall shear turbulence.

- Finally, if water quality aspects are of interest: what are the mass transfer characteristics between air and water?

A self-aerating flow configuration produces by mechanical action continuously air bubbles, which are subsequently carried away by the flow, if the transport capacity of the water flow is sufficiently high (Fig.1).

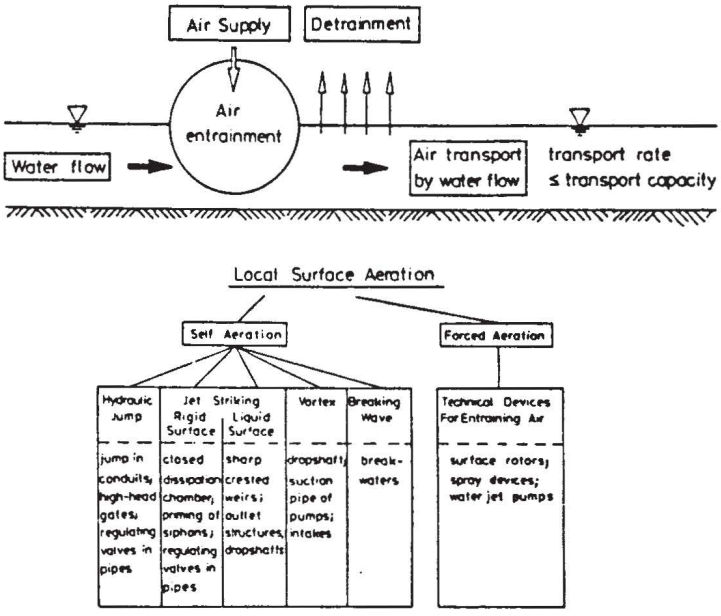

Fig. 1: Local air entrainment, detrainment and transport

All those bubbles which are entrained but cannot be transported by the flow will escape through the water surface (detrainment). This illustrates the interaction of air entrainment, transport capacity and detrainment. For a given configuration, the amount of entrained air will depend upon the approach water flow conditions as well as the conditions of air supply, which may be unrestricted (atmosphere) or governed by the flow through a duct system. On the other hand, the transport capacity of the system depends entirely upon the downstream water flow configuration. If the transport capacity is zero (as e.g. in stagnant or slowly flowing water bodies), then all entrained air will be discharged back into the atmosphere.

It follows from these remarks that in investigating local aeration and deaeration processes one has to consider not only the flow conditions of the water approach flow, but also the air supply conditions as well as the downstream transport conditions.

2 FLOW CONFIGURATIONS WITH LOCAL SELF-AERATION

2.1 DESCRIPTION

Free-surface flow configurations leading to local air entrainment are always connected with some form of surface discontinuity, such as a plunging jet or formation of a surface roller. A number of such flow configurations is sketched in Figs. 2 and 3. The basic difference to the situation of ambient surface aeration is the fact that in local aeration processes air may be entrained at a rate completely independent of the transport capacity: the latter is only of importance with regard to the question how far and for how long the air is kept in suspension. It depends upon the transport capacity of the flow, therefore, whether the entrained air is transported with the flow or rather quickly discharged into the atmosphere again, thus rendering the process of self-aeration as of local importance only.

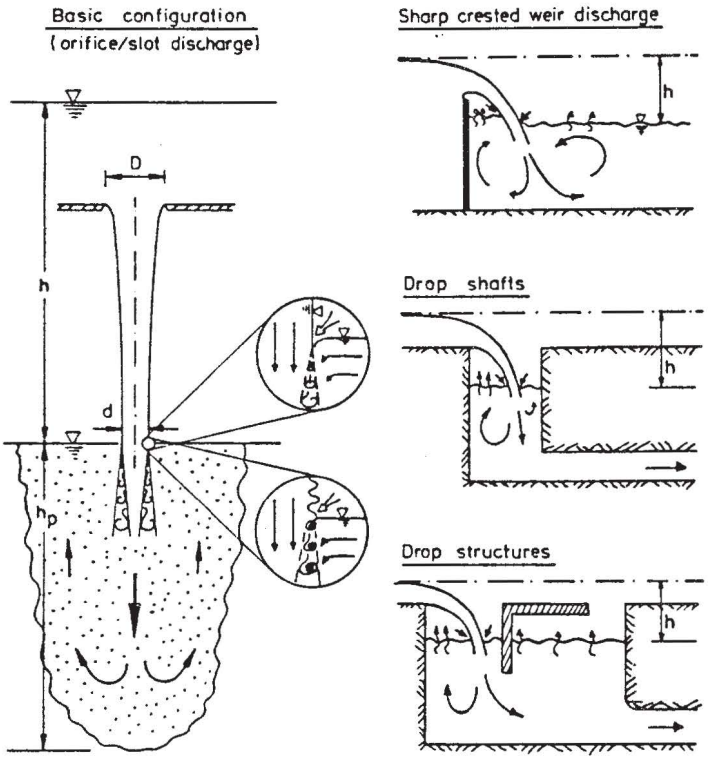

Fig. 2: Local air entrainment at "plunging-jet type" configurations

In Fig. 2, flow configurations of the plunging-jet type are illustrated. They are characterized by the fact that local air entrainment takes place at the intersection of the free jet with the water surface. Due to the momentum of the water jet, air is entrained in the free shear layer induced by the jet surface, which is a zone of intensive turbulence production. Plunging jet configurations are characterized by the fact that the momentum flux of the jet is predominantly in the vertical downward direction. The vertical momentum flux input will be directly counteracted by the buoyancy force of the entrained air, whereas the horizontal momentum flux components will remain essentially unchanged, since they experience no external force.

Fig. 3 shows flow configurations of the surface roller type, which are encountered

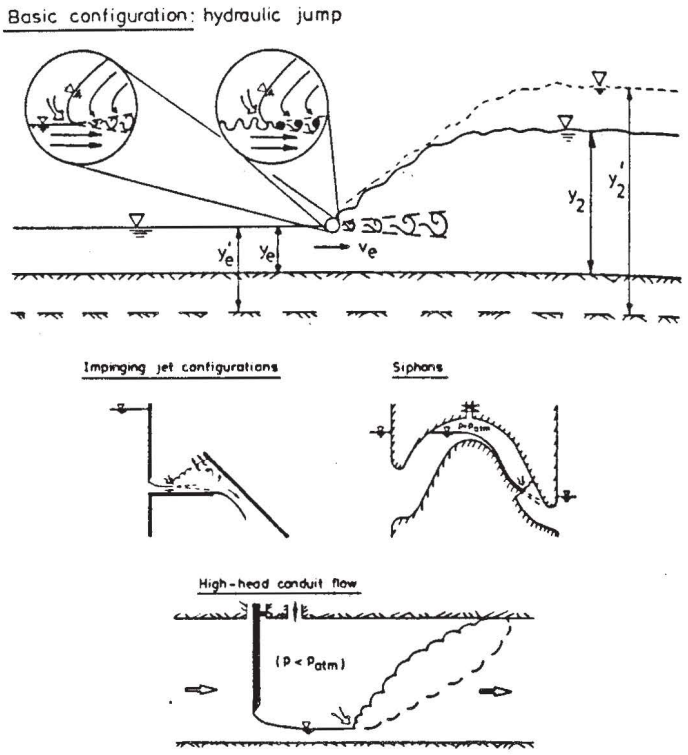

Fig. 3: Local air entrainment at "surface-roller type" configurations

most frequently in nearly horizontal flows. In these cases, local air entrainment takes place at the intersection of the free surface with the surface roller. Again, the air is entrained into the free shear layer which is characterized by intensive turbulence production. The entire flow field including the surface roller is governed by the momentum flux of the approach flow and by the downstream boundary condition.

There exists a number of other flow configurations which give rise to local air entrainment, but are not readily comparable with the two basic configurations described above. This includes high-head installations in conduits as well as aeration grooves on spillways and could be extended to the formation of vortices at intakes or the breaking of shallow-water waves. One basic difference is the fact that in these cases the air-entraining water flow configuration may vary considerably with the approach flow Froude number or the pressure conditions at the entraining surface: such effects have to be given careful attention before comparisons to other configurations can be made.

2.2 CONTROLLING CONDITIONS

The process of local air entrainment and detrainment is subject to several limiting conditions. We can distinguish an inception limit, entrainment limit, air supply limit and transport limit. Each one of these may be the controlling factor for local aeration. In comparing flow configurations of different geometry or size, attention has to be paid to all of these limits.

Inception limit: For a given flow configuration with a surface discontinuity, the flow conditions must be such as to generate a sufficiently large disturbance for air entrainment to occur. The inception limit depends strongly upon the fluid properties and characterizes the condition that

inertial reactions become large enough to overcome the resisting forces due to viscosity and surface tension. In general, a certain minimum velocity has to be exceeded, and the initiation of air entrainment is greatly enhanced by turbulent fluctuations of the approach flow.

Entrainment limit: The conditions of the approach water flow are governing the entrainment limit. These conditions are quantified by the Froude number. Depending upon the boundary geometry, a critical value of the Froude number must be exceeded to ensure the formation of a surface discontinuity at which air entrainment can occur (e.g. Fr > 1 for the hydraulic jump). For higher values of the Froude number, the approach flow, characterized by the velocity and turbulence distribution, provides the driving mechanism for the air entrainment. In most cases, the air entrainment process is not directly affected by the local boundary scale.

Air supply limit: Depending upon the flow configuration, air entrainment may occur at a free surface directly from the atmosphere with an unlimited supply of air at atmospheric pressure, or from a limited enclosed air space, which usually is connected to the atmosphere by an air duct (unless, like for siphons, the purpose is to evacuate the air volume). In this case, the supply of air to the point of entrainment into the water flow requires an air flow through the duct system which necessarily is connected with a pressure difference between the ends of the air duct. The subatmospheric pressure at the location of air entrainment must be resulting from the water flow conditions. As is sketched in Fig. 4, the maximum pressure difference occurs when the air duct is closed off. With increasing air supply, the pressure difference decreases (to zero for unlimited air supply). From this relation and the conditions of the air duct system, there results an operating point characterizing the resulting air supply rate and the corresponding pressure difference. This illustrates that the air supply system may become the limiting factor for local air entrainment.

Transport limit: The transport capacity of the flow is governed by the downstream flow conditions. It depends upon the flow velocity and turbulence as determined by the wall shear stresses /17/. An upper limit for air transport is given by the maximum possible air bubble concentration in the flow /2/.

2.3 DIMENSIONAL ANALYSIS

As a general frame for the discussion of scale effects, we can look at an overall dimensional analysis of the problem.

The dependent variables describing the air entrainment and detrainment process are air flow rates Q_a resp. q_a, resulting bubble sizes d_b, air concentrations and bulk dimensions of the air-water mixture, as well as trajectories and residence times of bubbles. In air flow rates, we have to distinguish the total rate of entrained air Q_{ae} from the specific flow rate q_{ae} per unit width of surface discontinuity, and in contrast to these the total and specific air transport rate Q_{at} resp q_{at} of the flow.

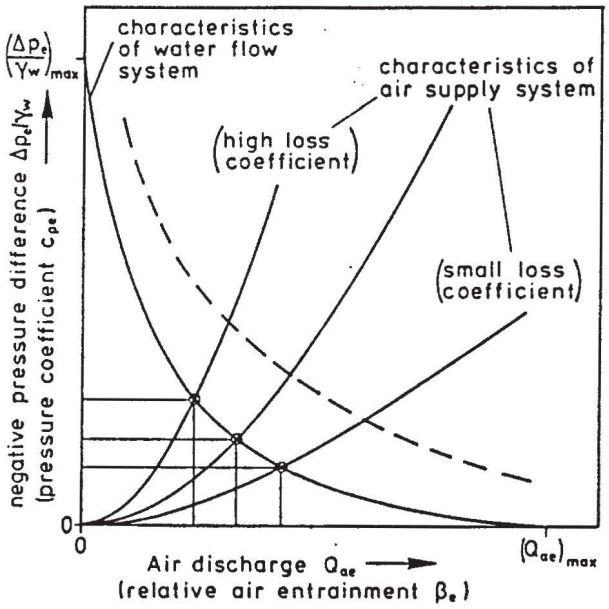

Fig. 4: Air supply control

All of these variables can be described in terms of the independent variables representing
- boundary geometry: reference length l_w;
- water approach flow: reference velocity v_w; (turbulence Tu);
- air supply system: pressure difference Δp_e;
- relevant fluid properties: ρ_w; g; η_w; σ_{wa};

This set of variables also describes the downstream flow conditions completely.

For the dependence of the specific rate of entrained air, for instance, we can now write

$$q_{ae} = f(\text{geometry}; l_w; v_w; (Tu); \Delta p_e; \rho_w; g; \eta_w; \sigma_{wa}) \qquad (1)$$

where the left hand side could be replaced by any other dependent variable of interest. A classical dimensional analysis leads to

$$\frac{q_{ae}}{v_w l_w} = f(\text{geom. ratios}; (Tu); \frac{\Delta p_e}{\rho_w v_w^2/2}; \frac{v_w}{\sqrt{g l_w}}; \frac{v_w l_w}{\eta_w/\rho_w}; \frac{v_w}{\sqrt{\sigma_{wa}/\rho_w l_w}}) \qquad (2)$$

or

$$\beta_e = \frac{q_{ae}}{q_w} = f(\text{geom. ratios}; (Tu); c_{pe}; Fr; Re; We) \qquad (3)$$

and alternatively by the rules of dimensional analysis /6/ to

$$\beta_e = f(\text{geom. ratios}; Tu; c_{pe}; Fr; Re; Z = \frac{g \cdot \eta_w^4}{\rho_w \cdot \sigma_{wa}^3}) \qquad (4)$$

and corresponding relationships for all other dependent variables. They represent the complete similarity requirements for local aeration processes.

As an alternative to the Weber number, which describes the relative importance of surface tension, the liquid parameter Z can be used. This parameter possesses the obvious advan-

tage that it contains neither the reference length nor the reference velocity. It is a function of the liquid properties alone and thus independent of the boundary scale and the flow velocity. For pure water, the value of the liquid parameter is ($Z \sim 10^{11}$); it will remain constant as long as the temperature and water quality remains unchanged.

2.4 MODEL INVESTIGATIONS

Studies of local air entrainment and detrainment rely heavily on experimental investigations on small scale models. Obviously, perfect dynamic similary can not be achieved, since the modelling parameters as derived from dimensional analysis cannot be satisfied simultaneously in a small scale model using the same fluids, i.e. air and water. It is often argued that the bubble sizes generated by free-surface aeration always exhibit about the same absolute size and hence violate in a small scale model both geometric similarity (ratio bubble size to boundary scale) and dynamic similarity (ratio of bubble rising velocity to water velocity). With use of the liquid parameter Z to describe the physical water quality, the complete similarity requirements are given by Eq. (4).

Restricting further considerations to a small scale model of geometric similarity, using water of the same quality as in the prototype (i.e. Z = const) and entraining from the atmosphere (i.e. $c_{pe} = 0$), this reduces to

$$\beta_e = f(Fr; Re; (Tu)) \qquad (5)$$

If according to the model law for free surface flows the Froude number is kept the same in model and prototype by proper choice of the model velocity scale, then the "scale effects" are embedded in the fact that the Reynolds number is not modelled correctly, and hence the turbulence characteristics of the flow. (The parameter "Tu" stands for the turbulence characteristics of the approach flow in the inlet section of the model). Quite general, since the model Reynolds number is always smaller than the corresponding value in the prototype, the effects of viscosity are exaggerated in the small scale model.

However, in fully turbulent flow the mean flow characteristics and the turbulence macroscale structure become independent of the Reynolds number, since the energy transfer in turbulence production from mean flow to macroscale turbulent eddies is dominated by inertial effects and viscosity becomes apparent only in the small scale dissipation of turbulent energy. Under such conditions, the resulting scaling requirement is reduced to the requirement that in either case the Reynolds number must be large enough so that fully turbulent flow conditions prevail. In prototype, this condition is usually met, and therefore this requires simply

$$Re_{model} \geq Re_t \qquad (6)$$

where Re_t marks the minimum Reynolds number for fully turbulent flow. If the local values of water velocity and depth or thickness at the entrainment location are used, then it is surmised that the value of Re_t is of the order of 10^5 or somewhat less.

3 AIR ENTRAINMENT

3.1 MECHANICS OF ENTRAINMENT

Most cases of local aeration have in common that the air entrainment takes place at a discontinuity of the free surface at which substantial velocity differences are encountered. In a hydraulic jump, for instance, the air is entrained exclusively at the toe of the surface roller. In impinging jets penetrating into a stagnant body of liquid, air is entrained along the circumference of the jet intersecting the free surface of the liquid. The essential local parameters governing the entrainment process are

- the velocity v_e (or velocity difference) at the line of air entrainment;
- the character (smoothness) of the water surface at the line of air entrainment, characterized by the intensity and scale of the turbulence of the approach flow, possibly also the air content of the approach flow;
- density ρ_w and gravity g.

If this common root of all configurations is used as a possible basis for comparison, then one can distinguish

- the "outer problem": how do these local characteristics depend upon the system parameters of the structure?
- the "inner problem": how does the air entrainment depend upon the local characteristics?

In looking at the "inner problem", a crucial point is the observation that there is no physically meaningful reference length involved in the air entrainment process.

The process of air entrainment can be visualized as air pockets being trapped between roller or liquid surface and inflow, which are then carried away in the downstream direction. The size and frequency of formation of such pockets can reasonably be expected to depend upon the differential velocity between roller and inflow, or - since the former is zero in the mean - upon the velocity of the inflow alone. Obviously, the boundary scale - for instance, the water depth or jet width - will in most cases have no influence upon the entrainment process unless it becomes small enough to be of the order of the enclosed air pockets. This fact can be used to deduce some information about the inception and entrainment limits.

3.2 INCEPTION LIMIT

The inception of air entrainment is governed by the condition that the free surface is penetrated and interrupted by the impinging flow. Air entrainment will commence when inertial and gravity forces override the resisting forces due to viscosity and surface tension. Therefore, the "critical" velocity v_c for onset of aeration will depend on the following fluid properties:

$$f(v_c; \rho_w; g; \eta_w; \sigma_{wa}) = 0 \qquad (7)$$

These can be grouped into two dimensionless parameters:

$$f\left(\frac{v_c^3}{g\,\eta_w/\rho_w}; \frac{g\,\eta_w^4}{\rho_w\,\sigma_{wa}^3}\right) = f\left(\frac{v_c^3}{g\,\eta_w/\rho_w}; Z\right) = 0 \qquad (8)$$

This means that the nondimensional critical velocity will depend upon the magnitude of

the liquid parameter Z, and if Z is kept constant (same water quality in model and prototype), the inception limit is characterized by

$$\frac{v_c^3}{g\,\eta_w/\rho_w} = \text{const} \approx (0.5 \div 1)\cdot 10^5 \qquad (9)$$

The order of magnitude given is a rough estimate taken from experimental evidence from plunging jets, which indicates that air entrainment commences at velocities of 0.8 to 1 m/s.

Equation 9 indicates that the inception limit neither corresponds to a constant Reynolds number nor to a constant Froude number.

3.3 ENTRAINMENT LIMIT

Considering the limiting case of fully turbulent flow (very high Reynolds numbers), one has to expect that the process of air entrainment will finally become independent of viscosity, since the large-scale turbulence is governed by inertial reactions alone. In these cases the amount of air entrainment per unit length of surface discontinuity becomes

$$q_{ae} = f(v_e; \rho_w; g) \qquad (10)$$

This leads to a single dimensionless parameter, which hence must necessarily attain a constant value:

$$\frac{q_{ae}}{v_e^3/g} = \text{const} \qquad (11)$$

and from this, with ($q_w = v_e\ y_e$) there follows

$$\frac{q_{ae}}{q_w} = \beta_e = \text{const}\ \frac{v_e^2}{g\ y_e} = \text{const}\cdot Fr^2 = k_e \cdot Fr^2 \qquad (12)$$

with k_e defined as an "entrainment coefficient". In fully turbulent flow, k_e should be constant and hence the relative air entrainment directly proportional to the square of the local Froude number.

An example of air entrainment governed by this condition is shown in Figs. 5 and 6. Renner's experiments on a jet impinging on a wall clearly confirm Eq. (12) over a wide range of Froude numbers; deviations from this relation are attributed to approaching the transport limit of the configuration.

In the general case, the viscosity η_w and the turbulence characteristics Tu of the approach flow have to be added to the list of independent variables in Eq. (10). The result of the dimensional analysis is then

$$\beta_e = k_e(Re; Tu)\cdot Fr^2 \qquad (13)$$

The factor Tu summarizes all relevant conditions of the approach flow which may be expected to have an influence on the mechanics of the entrainment process. This includes the velocity distribution over the cross section, flow curvature effects, turbulence intensity and scale, and air content in the approach flow.

3.4 SCALING CONSIDERATIONS IN FROUDE MODELS

The scaling relationship Eq. (5) can be plotted, for given approach flow turbulence Tu, in general form as a graph of lines of constant β_e in a Fr-Re plane. Such a diagram is sketched in Fig. 7. Since both Fr and Re

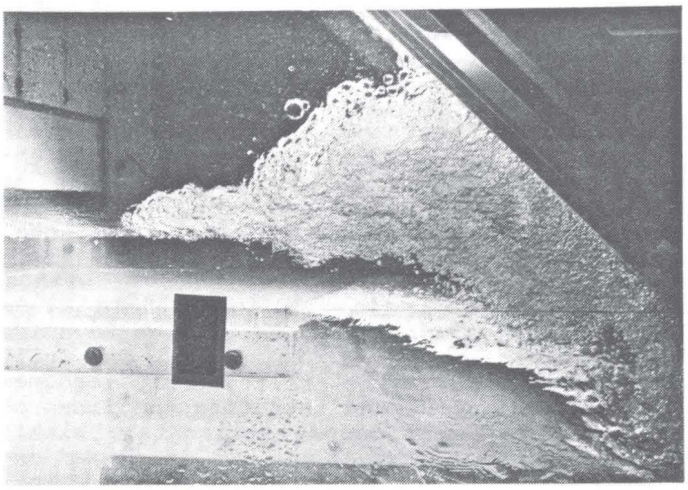

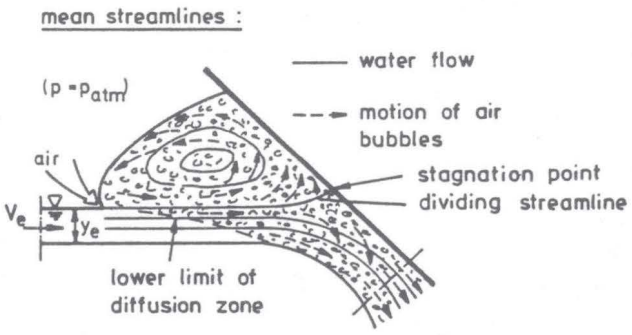

Fig. 5: Air entrainment in a jet impinging on a wall /14/

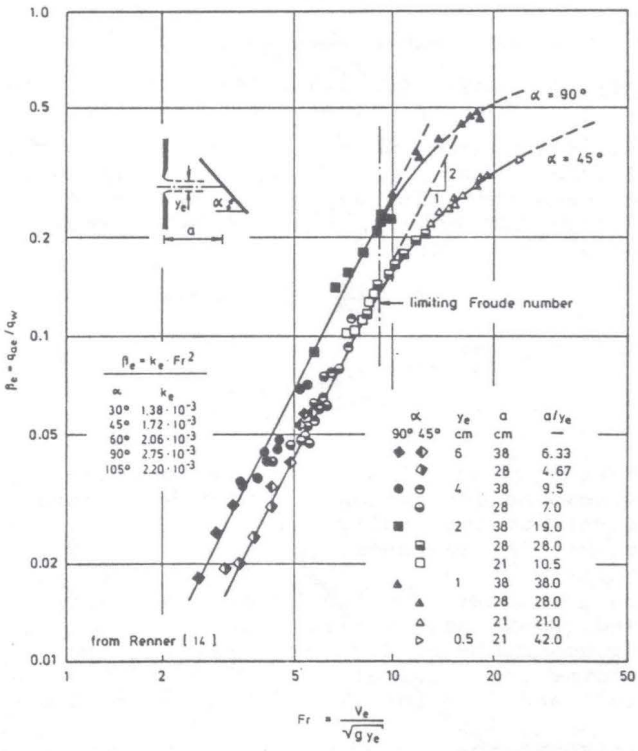

Fig. 6: Some experimental results for horizontal jets /14/

are based on the same reference quantities, lines of constant velocity and of constant reference lengths can be identified in this plane.

Information about the form of the relationship Eq. (5) can be obtained from consideration of the asymptotic behaviour at the inception limit and the entrainment limit under fully turbulent conditions. According to Eq. (9), the inception limit will plot as a line of constant v_e with a slope of (- 1/2) in the logarithmic Fr-Re plane. The asymptote for very large Reynolds numbers is given by Eq. (12). In fully turbulent flow, the relationship becomes independent of Re and therefore the lines of constant β_e must become horizontal. Within these limiting conditions, it is to be expected that lines of constant β_e will exhibit a general shape as indicated in Fig. 7 for any given flow configuration.

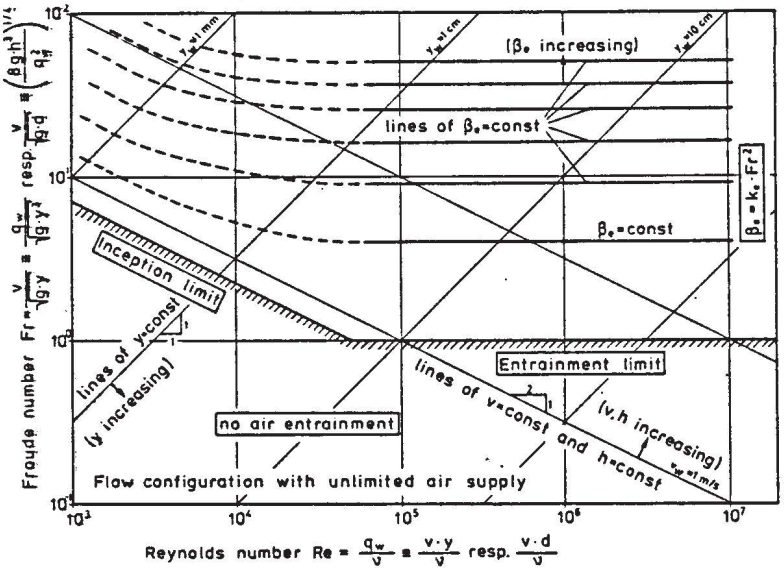

Fig. 7: Suggested functional relationship for the relative air entrainment β

The conditions of fully turbulent flow are reached when the local Reynolds number exceeds the value Re_t as defined in Eq. (6). For Froude models, the following relationship can be derived

$$Fr \cdot \left(\frac{\sqrt{g}}{\eta_w/\rho_w}\right) l_e^{3/2} \equiv Re \geq Re_t \qquad (14)$$

and from this

$$l_e \geq \left[\frac{Re_t}{Fr} \cdot \left(\frac{\eta_w/\rho_w}{\sqrt{g}}\right)\right]^{2/3} \qquad (15)$$

For a given flow configuration, Eq. (15) allows an estimation of the model dimensions required for fully turbulent flow. This means, for instance, for models of hydraulic jumps with (Fr_e > 1), that Eq. (15) should be satisfied for the lower limit (Fr = 1) and hence necessarily also for all higher Froude numbers. This requires minimum water depths for critical flow of 10 cm for ($Re = 10^5$) and 2 cm for ($Re = 10^4$), respectively.

It seems that in flow configurations of the "plunging jet" type, the flow often is far from fully turbulent and therefore the "inception limit" is markedly noticeable in plots of β_e versus Froude number. On the other hand, in "surface roller" configurations usually Reynolds numbers are much larger and fully turbulent flow is more often encountered, so that here direct correlations of β_e with Fr are more promising.

4 TRANSPORT AND DETRAINMENT

4.1 TRANSPORT CAPACITY

The transport capacity of the water flow depends primarily upon the ratio between water velocity v_w and bubble rise velocity v_b. In stagnant water bodies ($v_w \ll v_b$), the transport capacity is zero. The air bubbles will rise due to their buoyancy to the surface and escape. In slowly flowing water ($v_w \approx v_b$), the entrained air bubbles are displaced by the water flow, while the flow field may be changed drastically by the presence of the air bubbles.

In open channel high-speed flows ($v_w \gg v_b$), the transport capacity increases with increasing velocity and turbulence intensity of the water flow. The transport capacity is characterized by an equilibrium situation between the rising tendency of the bubbles and the counteracting mixing effect of the turbulent fluctuations in a concentration gradient, quite analog to the transport of suspended solids (although bubbles do show several distinct differences to solid particles).

In closed conduit flow, the transport capacity is additionally dependent upon the orientation of the flow towards the vertical, which marks the direction of the buoyancy force. Obviously, the transport capacity will be a maximum in vertically upward flow and a minimum for vertically downward flow.

Whenever the local air entrainment exceeds the transport capacity of the subsequent channel or conduit, local detrainment will take place. The resulting net detrainment can be expected to be proportional to the excess amount of air exceeding the transport capacity. A hydraulic jump, for instance, entrains a considerable amount of air locally, but because of little or no air transport capacity discharges most of it back into the atmosphere through the surface roller, so that after a short distance downstream the air content of the flow is almost zero again (Fig. 8).

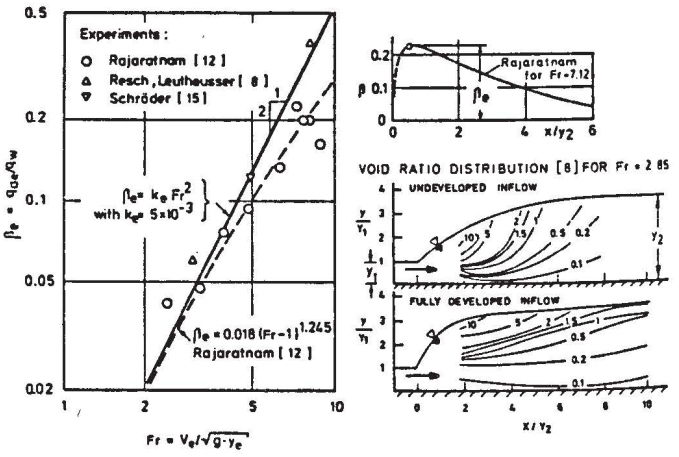

Fig. 8: Detrainment in a hydraulic jump /13/

If the transport capacity is exceeded in conduit flows, then the "detraining" air will collect at the top of the conduit and form air pockets of increasing size. Depending upon the flow velocity and the inclination of the conduit, these pockets may move in the direction of flow or against it,

which results in unsteady flow conditions with considerable pressure fluctuations and flow instabilities in the system ("blowout" or "blowback").

4.2 BUBBLE FORMATION

The process of air entrainment involves the entrapment of an air volume at the surface discontinuity, the breakup of the entrapped air volume into an array of bubbles, and the subsequent transport by the flow, during which the bubble size distribution may change due to coalescence or breakup of individual bubbles. Whereas the entrapment and initial breakup are governed by inertial and gravitational forces and hence Froude number dependent, the bubble transport is governed by the turbulence characteristics and hence the Reynolds number of the flow.

As a possibility for comparison, the breakup of a continuous air jet discharging from a nozzle into a water body has been studied by many investigators. Analytical consideration on instability and breakup of air pockets by Rayleigh have been verified experimentally /6/. At injection of a continuous air jet through a nozzle into an otherwise stagnant water body, the air jet immediately breaks up into an array of bubbles which range in diameter from almost zero up to a maximum value, which depends upon the air discharge and gravitational acceleration /6/:

$$d_{b_{max}} = (1.138 \div 1.72)\,(Q_a^2/g)^{1/5} \qquad (16)$$

In free-surface aeration, there will also result a mixture of bubbles up to a certain maximum size; no information is available, however, about the magnitude of the resulting upper limit.

Numerous visual observations and some measurements of bubble sizes in a turbulent flow have shown that the majority of the larger bubbles are in the range of 1 to 10 mm, and that the mean bubble diameter decreases with increasing turbulence. Some examples of measured bubble size distributions in air bubble screens are shown in Fig. 9. From these observations one may suspect that turbulent flows of air-water mixtures should finally reach a state of equilibrium with a certain turbulence structure and a corresponding bubble size distribution.

4.3 BUBBLE SLIP VELOCITIES

Air bubbles of finite size (diameter d_b) always exhibit a slip velocity v_b relative to the sorrounding water. To a reasonable degree of approximation, this slip velocity corresponds to the bubble rising velocity of a single bubble in an infinite fluid otherwise at rest. The flow field can therefore be considered as a combination of the water flow field with the bubble slip velocity superimposed.

The behaviour of a single gas bubble in a liquid has been studied extensively and is described e.g. in /6/. A dimensional analysis for the bubble rise velocity v_b of a bubble of diameter d_b yields

$$c_d \equiv \frac{4g\,d_b}{3v_b^2} = f\left[Re \equiv \frac{v_b d_b}{\eta_w/\rho_w} ; Z \equiv \frac{g\,\eta_w^4}{\rho_w \sigma_{wa}^3}\right] \qquad (17)$$

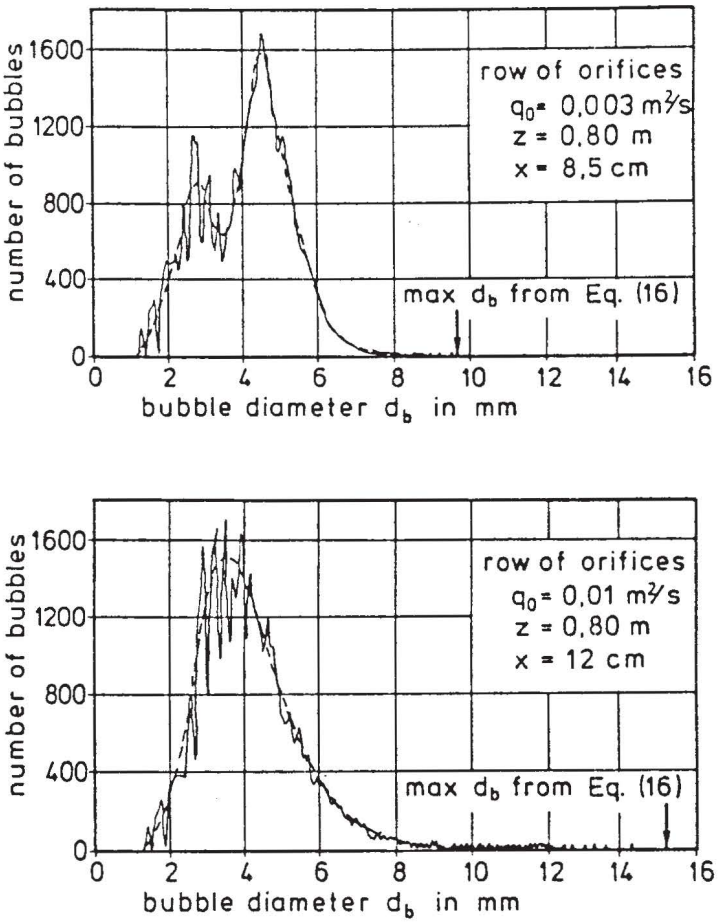

Fig. 9: Examples of resulting bubble size distributions from /1/

The quantitative relation between these parameters is given in Fig. 10. This diagram shows a nearly universal relation between c_d and Re, in which the influence of the liquid parameter Z is pronounced merely in the region of Reynolds numbers between 10^2 and 10^3. This indicates that for Reynolds numbers smaller than 10^2 (small gas bubbles) and larger than 10^3 (large air bubbles) the c_d-versus-Re relation can be considered as universal and valid for any kind of gas or liquid, whereas in the intermediate region ($10^2 < Re < 10^3$), the liquid parameter plays an important role.

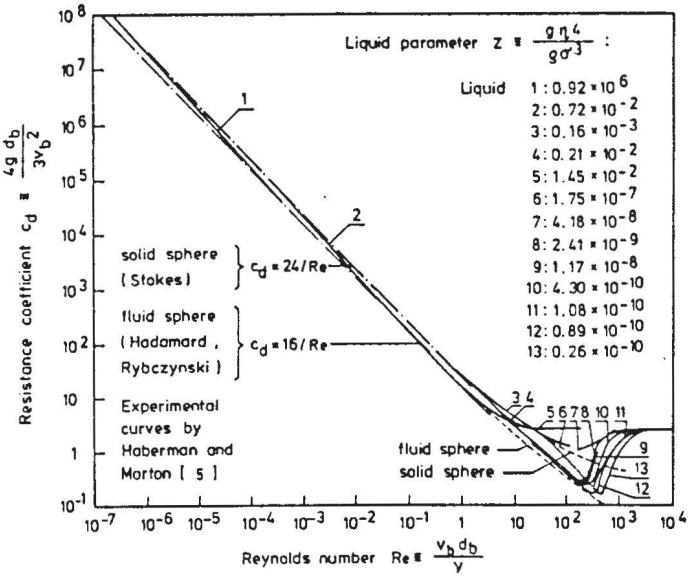

Fig. 10: General resistance diagram for gas bubbles in liquids /6/

4.4 BUBBLE-INDUCED WATER FLOW

The entrained air bubbles exert a buoyancy force on the surrounding water, which gives rise to a bubble-induced water flow. This can best be illustrated by considering a bubble plume generated by injection of compressed air at the bottom of a stagnant water body. In this case, the resulting mean and turbulent flow field is entirely due to the buoyancy of the induced air discharge and to the dynamics of the bubble swarm (purely bubble-induced turbulence).

The flow field of air and water in bubble plumes /6/ is characterized by the fact that the vertical momentum flux of the induced water flow increases with upward distance from the air source due to the action of the bubble buoyancy. The buoyancy force input per unit time is given by the amount of entrained air:

$$B = (\rho_w - \rho_a)\, g\, Q_a \approx \rho_w g\, Q_a \qquad (18)$$

and with this the vertical momentum flux $M_{w,z}$ can be expressed as

$$\frac{dM_{w,z}}{dz} = B - F(v_b) \qquad (19)$$

If the bubbles would be infinitely small (i.e. zero slip velocity and hence also $F(v_b) = 0$), then the flow field should correspond to the classical buoyant plume. However, bubbles of finite size do exhibit a slip velocity v_b relative to the surrounding water, which results in a correspondingly smaller increase of the water momentum flux. The acting buoyancy force B is partly used up for moving the air bubble through the liquid (resistance force $F(v_b)$ to slip velocity) and only the remaining part acts to increase the water momentum flux $M_{w,z}$.

This illustrates the importance of the bubble sizes for the concentration and flow field: the larger the bubbles, the higher the slip velocity v_b and the less pronounced the induced water velocity.

In contrast, the horizontal momentum flux of the water flow remains essentially unaffected by the presence of the air bubbles. Due to their negligible density, the air bubbles are transported laterally by the water flow without considerable slip velocities. The only noticeable change for the horizontal flow components will therefore be, in high air concentrations, an effect upon the local mixture density to be considered in the momentum equation.

It follows from these considerations that the most pronounced effects of air bubbles upon the water flow are to be expected in predominantly vertical flow configurations, such as plunging jet or drop shaft arrangements, but play a lesser role in predominantly horizontal flows. As an illustrative example for the drastic effects that entrained air can have on the water flow field, two flow situations in a drop structure are shown in Fig. 11, which are described in detail in /7/

4.5 SCALING CONSIDERATIONS IN FROUDE MODELS

The question of transport and detrainment of air is very closely linked to the question of the resulting bubble sizes. The argument that in models bubble sizes are proportionally too large would hint at scale effects in the sense that detrainment is too large in the model and hence transport too small. This ties in with the fact that due to the lower turbulence level (smaller Reynolds number) the transport capacity in the model is expected to be smaller than in the prototype.

Since the resulting bubble size distribution depends upon the turbulence characteristics of the flow (and hence Reynolds number), the same is to be expected for the bubble transport and detrainment.

A first step to quantify the local detrainment process is given by Thomas /16/. For flow configurations with a surface roller, he considers the dividing streamline between the main flow and the recirculating roller: All bubbles above the dividing streamline contribute to local detrainment, all those below are transported away. For quantification, a simplified model of the turbulence structure of the flow is used /16/.

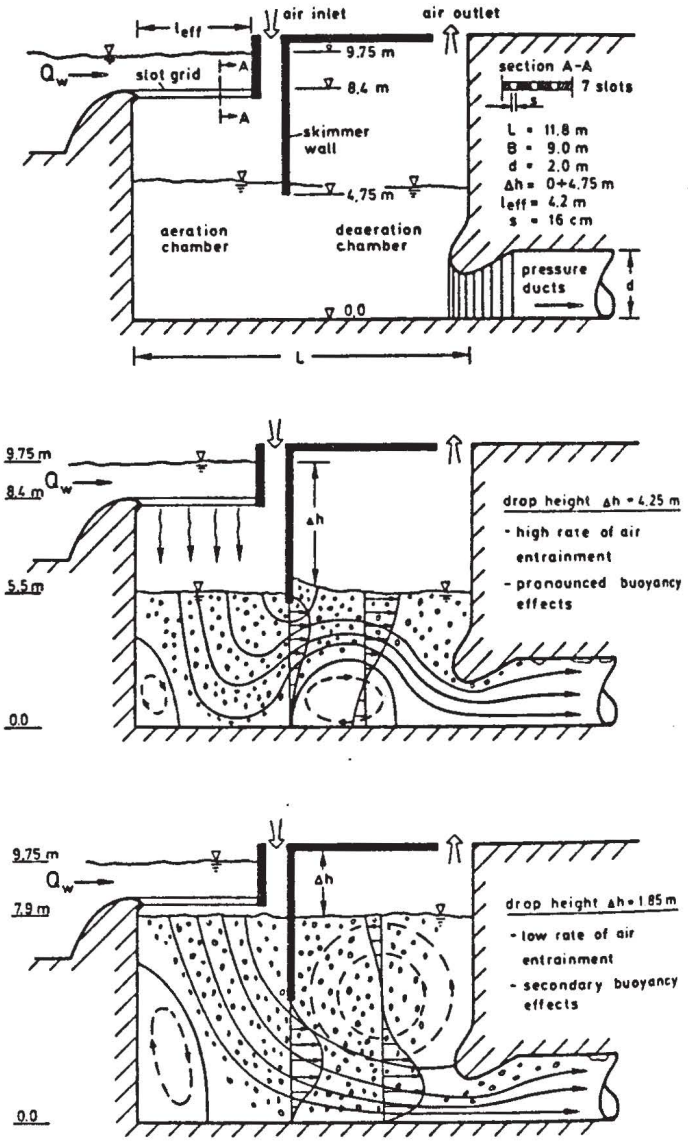

Fig. 11: Effects of air buoyancy upon the water flow field: example from /7/

5 MASS TRANSFER

5.1 ADDITIONAL PARAMETERS

For water quality purposes, local aeration processes are often welcome as means to increase the oxygen content of the water. In these cases it is of interest to know the rate of mass transfer between air and water. This depends upon the concentration difference between air and water, upon the contact area, i.e. total surface area of the bubbles, and upon the surface renewal rate, i.e. turbulent mixing, contact times, and bubble trajectories. The process of reoxygenation can be considered in three consecutive steps:

- mechanics of air entrainment;
- mechanics of air transport away from the entrainment location, and
- transfer of oxygen from the air bubbles into solution.

The first two steps depend upon hydrodynamics alone, whereas the third step represents the phase of the process which depends upon the water quality, such as temperature, initial dissolved oxygen content, salinity, and degree of water pollution.

The bubble trajectory or residence time will be governed by the same parameters as the air entrainment. Hence all similarity considerations given so far will also pertain to mass transfer problems. In particular, the turbulence characteristics (scale and intensity) of the flow and hence the Reynolds number may have a marked influence upon the bubble transport.

The mass transfer is described by the increase in concentrations in the water while passing the installation. For oxygenation, this is usually expressed in terms of the reoxygenation rate r in terms of oxygen concentrations c as follows:

$$r \equiv \frac{c_{saturation} - c_{upstream}}{c_{saturation} - c_{downstream}} = \frac{\text{deficit upstream}}{\text{deficit downstream}} \geq 1 \qquad (20)$$

This coefficient r will again depend upon the same parameters as given by Eq. (5) for the air entrainment rate, as well as upon the additional parameters governing the mass transfer rate, such as water temperature, water quality, salt content and pressure conditions. Therefore, when comparing results on mass transfer from various investigations, one has to reduce the data to "standard conditions" with respect to these parameters.

As one example of a generalized data presentation on the basis described above, Markofsky and Kobus /9/ have developed a diagram for sharp crested aerated rectangular weirs discharging into a deep plunging pool. In Fig. 12, all available model and field data are plotted, which describe in a consistent fashion the relation between observations at various scales.

5.2 SCALING CONSIDERATIONS

A discussion of Fig. 12 illustrates well the scaling considerations for plunging jets. In the laboratory, for low flow rates and low heights of fall (lower left corner of Fig. 12), surface tension prevents air entrainment and therefore reoxygenation from occuring. The effect of surface tension is overcome as a result of an increase in the flow rate or height of fall or both. Air is entrained to greater depths and, with increasing turbulence, is broken into finer and finer bubbles. Both effects increase the efficiency of the gas transfer process. Thus, in this region reoxygenation increases with both q_w and h.

In the fully turbulent field situation (right-hand side of Fig. 12), Eq. (12) governs. The amount of air entrainment is determined by the impingement velocity v_e at the nappe which is a function of the height of fall h only. Thus, the same quantity of air will be entrained for the same height or fall regardless of the flow rate. Therefore, with increasing water flow rate, there is less air per volume of water available and thus the reoxygenation rate decreases. In the logarithmic parameter presentation of Fig. 12, lines of constant h are given by straight lines with a slope of (- 1/2), i.e. parallel to the dashed line. Proceeding along such a line towards higher flow rates, i.e. to the right, shows that for a constant height of fall r decreases with increasing water discharge in the large-scale field situation. On the other hand, r increases with increasing height of fall at a given water flow rate (vertical line).

Considering small scale Froude models in Fig. 12, one proceeds along a horizontal line (Fr = constant) from left to right (to large Re) in going from a small scale Froude model to the prototype situation. It is seen that the reoxygenation rate r will necessarily be smaller in the model than in the prototype. This is mainly due to the fact that the small model does not correctly scale the air entrainment rate, which depends primarily upon the height of fall h. Laboratory experiments for the determination of reoxygenation rates r have therefore often been performed at prototype dimensions of h. Historically, the results of such studies have been presented in equations in which r is a function of h only (see references in /9/) without consideration of the flow rate q_w. Such equations will plot as straight lines with a slope of (- 1/2), i.e. parallel to the dashed line in Fig. 12: in these cases predictions of r from laboratory studies at low flow rates lead to overestimations of r for high flow rates at the same height of fall /9/.

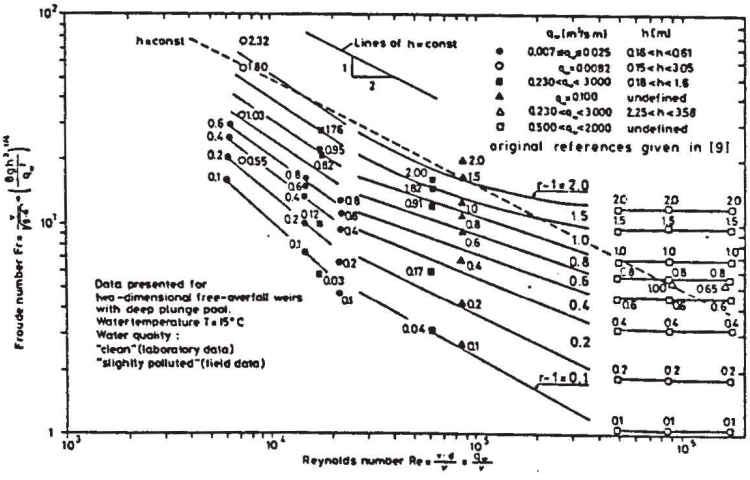

Fig. 12: Unified presentation of weir aeration data /9/

6 CONCLUSIONS

The highly complex phenomenon of local air entrainment and detrainment may be controlled by the approach flow, by the air supply or by the downstream transport capacity: all of these have to be considered carefully in evaluating model studies for prototype conditions.

The mechanism of air entrainment depends upon the approach flow conditions and is characterized by an inception limit (critical velocity) and by an entrainment limit. Scale considerations for Froude models should be based on the local Reynolds number at the entraining cross section.

The flow conditions in the air supply system govern the local pressure at the entrainment point, which may control the air entrainment rate. This necessitates in hydraulic model studies that the air supply system has also to be modelled correctly.

In low velocity flows, air transport and detrainment is strongly influenced by the bubble size distribution, which in turn is governed by the turbulence characteristics of the flow. Since these are Re-dependent, deviations in the resulting flow fields and concentration distributions are to be expected between Froude model and prototype.

Since our knowledge about local aeration is still scarce, further research and experimental investigations are needed. It is hoped that a systematic approach and a generalized evaluation of available data will lead to a better understanding and quantitative assessment of the processes involved.

REFERENCES

/1/ Barczewski, B: Neue Meßverfahren für Wasser-Luftgemische und deren Anwendung auf zweiphasige Auftriebsstrahlen. Heft 45. Mitteilungen des Instituts für Wasserbau, Universität Stuttgart, 1979

/2/ Brauer, H.: Grundlagen der Einphasen- und Mehrphasenströmungen. Verlag Sauerländer, Aarau und Frankfurt am Main, 1971

/3/ Ervine, A.: Scaling Relationship for a Two-Dimensional Vertical Dropshaft. Proc., BHRA Conference on Hydraulic Modelling of Civil Engineering Structures. Coventry, England, September 1982

/4/ Falvey, H.T.: Air Water Flow in Hydraulic Structures. Water Resources Techn. Publication. Engineering Monograph No. 41. US Department of Interior, 1980

/5/ Haberman, W.L. and Morton, R.K.: An Experimental Study of Bubbles Moving in Liquids. Proceedings ASCE. Vol. 80. No. 379 - 427, 1954

/6/ Kobus, H.: Bemessungsgrundlagen und Anwendungen für Luftschleier im Wasserbau. Heft 7. Schriftenreihe "Wasser und Abwasser in Forschung und Praxis", Erich Schmidt Verlag. Berlin, 1973

/7/ Kobus, H. and Westrich, B.: An Example of a Combined Discharge-Control and Aeration Structure. Proc. XX. Congress IAHR. Moscow, USSR. September 1983

/8/ Leutheusser, H.J., Resch, F.J. and Alemu, S.: Water Quality Enhancement Through Hydraulic Aeration". Proc. 15th Congress IAHR, Istanbul, Turkey, September 1973

/9/ Markofsky, M. and Kobus, H.: Unified Presentation of Weir-Aeration Data. ASCE Journal of Hydraulic Research, April 1978

/10/ Novak, P.: Luftaufnahme und Sauerstoffeintrag an Wehren und Verschlüssen. In: DVWK Schriftenreihe "Natur- und Modellmessungen zum künstlichen Sauerstoffeintrag in Flüsse". Heft 49. Paul Parey Verlag. Hamburg, 1980

/11/ Pinto, N.L. de S., Neidert, S.H.: Air Entrainment Through Aerators - Mechanism and Air Flow Evaluation. Proc. XX IAHR Congress. Moscow, USSR. September 1983

/12/ Rajaratnam, N.: An Experimental Study of Air Entrainment Characteristics of the Hydraulic Jump. Journal of the Institution of Engineers of India. Vol. 42. No. 7. March 1962

/13/ Rao, N.S.L. and Kobus, H. (Editors): Characteristics of Self-Aerated Free-Surface Flow. Schriftenreihe "Wasser und Abwasser in Forschung und Praxis". Erich Schmidt Verlag. Berlin. 1975

/14/ Renner, J.: Lufteinmischung beim Aufprall eines ebenen Wasserstrahls auf eine Wand. Dissertation. Universität Karlsruhe. 1973

/15/ Schröder, R.: Die turbulente Strömung im freien Wechselsprung. Mitteilungen. Institut für Wasserbau und Wasserwirtschaft. TU Berlin, Heft 59. 1963

/16/ Thomas, N.: Air Demand Distortion in Hydraulic Models: Experimental Evidence of Bi-Modal Structure in Air Entraining Flows and a Scaling Analysis of Detrainment with Special Applications to Siphon Priming. Proc. BHRA Conference on Hydraulic Modelling of Civil Engineering Structures. Coventry, England. September 1982

/17/ Wood, I.R.: The Uniform Region in Self-Aerated Flow. Proc. ASCE Hydraulics Division. Vol. 109. No. 3. March 1983